Journal of Nuclear Materials 415 (2011) S860–S864

Contents lists available at ScienceDirect

Journal of Nuclear Materials

journal homepage: www.elsevier.com/locate/jnucmat

Interpretation of divertor Langmuir probe measurements during the ELMs at JET

D. Tskhakaya [a,b,*,1,2], S. Jachmich [a,c], T. Eich [a,d], W. Fundamenski [a,e], JET EFDA contributors [a,3]

[a] JET-EFDA, Culham Science Centre, OX14 3DB Abingdon, UK
[b] Association EURATOM-ÖAW, University of Innsbruck, A-6020 Innsbruck, Austria
[c] Laboratory for Plasma Physics, EURATOM-Association 'Belgian State', B-1000 Brussels, Belgium
[d] IPP-EURATOM Association, D-85748 Garching, Germany
[e] EURATOM-UKAEA Fusion Association, Culham Science Centre, Abingdon OX14 3DB, UK

ARTICLE INFO

Article history:
Available online 27 November 2010

ABSTRACT

We present results of massively parallel kinetic simulations of the triple Langmuir probes at JET. These results indicate that the probes under certain conditions, e.g. during ELMs, can significantly under/over estimate the electron temperature.

1. Introduction

Langmuir probes (LP) are frequently used for measuring the electron temperature (T_e) and estimation of plasma (n) and energy flux (q) densities in the fusion plasma edge (i.e. SOL – Scrape-off Layer). The disadvantage of these measurements is the sensitivity to the deviation of the electron velocity distribution function (EVDF) from the Maxwellian distribution [1]. This is the consequence of the fact that the properties of the sheath in front of the probe surface are strongly influenced by the super-thermal electrons (see [2] and references therein). There are different processes in the SOL leading to de-Maxwellization of the EVDF: inelastic collisions of electrons with neutrals and impurity, fast time scale processes like ELMs (Edge-Localized Modes), blobs and so on. There are number of observations indicating that under some circumstances the T_e measured by LP can significantly deviate from the actual T_e in the SOL, e.g. in [3] are reported that during ohmic heating at ASDEX the T_e measured by LP is at least by the factor of two higher than one measured by Thomson scattering; in [4] is reported on LP measurements showing $T_e \sim 5$ eV, while the quantitative fluid modeling predicts $T_e \sim 1$ eV. Another example is a T_e measured during the ELMs: it is systematically underestimating the corresponding fluid [5] as well as kinetic [6] modeling results. A typical example is the LP measurement at JET indicating increase of the temperature during the ELM $\Delta T_e \sim 10$–50 eV [7], while the corresponding kinetic modeling showing ΔT_e to be of the order of 100 eV [8,9]. Number of attempts has been made in order to estimate effects of the super-thermal electrons on LP measurements by assuming bi-Maxwellian EVDF [10–12].

The aim of this work is to perform quantitative kinetic modeling of LP measurements at JET using EVDFs obtained in a self-consistent manner. The inter-ELM and ELMy SOLs are considered separately.

2. Description of the kinetic model

Triple Langmuir probes (TP) are used at JET for measuring of divertor plasma parameters in the ELMy SOL [7]. The TP consists of three single probes and measures simultaneously three parameters (see [1]): the ion saturation current (J^i_{sat}), the floating potential (V_{fl}) and biasing potential of the "positive" probe (V_+). Plasma parameters are obtained according to the following expressions,

$$T_e^{TP} = \frac{V_{fl} - V_+}{\ln 2}, \quad n = J^i_{sat}/eC_s, \quad q_{div} = \gamma J^i_{sat} T_e \sin(\alpha)/e, \quad C_s = \sqrt{2T_e^{TP}/M_i}, \tag{1}$$

where we assume that $T_e \ll V_{fl}$ and surface areas of the positive and "negative" probes are equal [1]. n ($\equiv n_i \approx n_e$), "e", q_{div} and α are the plasma density, unit charge, the divertor heat flux and the angle between the magnetic field and divertor surface, respectively; γ is the sheath heat transmission coefficient, which is usually chosen to be eight (e.g. see [8]). Here and below the temperatures are given in eV and voltage in V.

For simulation of the probe measurements we use the quasi-2D massively parallel PIC/MC code "BIT1 parallel" allowing large scale modeling of the SOL with finest resolution in time and space (down to the electron gyro-rotation). Simulation details are given below. Here we just note that one of the direct outputs of the simulations are the VDF of plasma particles $f_{e,i}(x, V_{||}, t)$, where x and $V_{||}$ are the poloidal coordinate and the parallel velocity respectively. The TP is "simulated" in a following way. Using current conservation for

* Corresponding author. Address: Technikerstrasse 25/II, A-6020 Innsbruck, Austria.
E-mail address: david.tskhakaya@uibk.ac.at (D. Tskhakaya).
[1] Permanent address: Andronikashvili Institute of Physics, 0177 Tbilisi, Georgia.
[2] Presenting author.
[3] See the Appendix of F. Romanelli et al., Proceedings of the 22nd IAEA Fusion Energy Conference 2008, Geneva, Switzerland.

0022-3115
doi:10.1016/j.jnucmat.2010.10.090

floating and positive/negative probes (see [1]) we obtain the following expressions:

$$J^i_{sat} \equiv \int_0^\infty V_{||} f_i(x, V_{||}, t) dV_{||} = \int_{\sqrt{2V_{fl}/m_e}}^\infty V_{||} f_e(x, V_{||}, t) dV_{||},$$
$$2J^i_{sat} = \int_{\sqrt{2V_+/m_e}}^\infty V_{||} f_e(x, V_{||}, t) dV_{||} + \int_{\sqrt{2(V_+ + U)/m_e}}^\infty V_{||} f_e(x, V_{||}, t) dV_{||}, \quad (2)$$

where U is the biasing potential of the TP. The electron and ion VDF from the simulation are substituted in the system (2), which is solved in order to obtain V_{fl} and V_+. Finally, these values (together with some chosen U) are substituted in the expressions (1) giving T_e^{TP} and n measured by the simulated TP.

The BIT1 parallel represents an electrostatic PIC + Monte Carlo code for massively parallel simulations of the edge plasmas [13,14]. Plasma, neutral and impurity particles are treated in 1D3 V, 2D3 V and quasi-2D3 V approximation, respectively (nDmV means n-dimensional in usual and m-dimensional in velocity space). For SOL simulation a slab geometry is used representing generalisation of previous models [9,15], see Fig. 1. In order to speed up the simulation we used a reduced model consisting of electrons, D^+ and C^+ ions, and D and C atoms. Plasma particles (electrons and D^+ ions) are injected in the source region mimicking cross-field transport through the separatrix. The source has a smooth shape $S = S_0 \cos(\pi(x_{omp} - x)/L_s)$, where $x_{omp} = 5$ m, L_s are the poloidal position of the outer mid-plain and the half-extension of the source region, respectively. For stationary and ELMy SOL we choose $L_s = 2$ m and $L_s = 0.75$ m. The strengths of the source, S_0, for the stationary and ELMy SOL are obtained from total particle and energy balance, respectively.

Plasma particles absorbed at the divertor plates cause emission of atoms. Neutrals reaching the outer wall or crossing the separatrix are removed from the simulation. The radial transport of neutrals as well as the impurity diffusion (see below) are introduced just in order to account for particle losses due to radial transport. Plasma parameters correspond to the flux tube adjacent to the separatrix.

Atomic physics and plasma-wall interaction model used in BIT1 is described in [16]. "Shorting" factor is 25 (see [9]) and the number of cells along the poloidal direction is 12,000. In the present model we made number of updates:

i. We implemented sputtering of C atoms (including self-sputtering). The recycling coefficient is given below:

$$Y = Y_{ch} + Y_{ph}, \quad Y_{ch} = 0.01,$$
$$Y_{ph} = \frac{A}{\cos\alpha} \frac{3.441\sqrt{E_0/E_{TF}}\ln(E_0/E_{TF} + 2.718)}{1 + 6.355\sqrt{E_0/E_{TF}} + E_0/E_{TF}(6.882\sqrt{E_0/E_{TF}} - 1.708)} \left(1 - \frac{E_{th}}{E_0}\right)^{8/3}, \quad (3)$$

where Y_{ch} and Y_{ph} correspond to the chemical and physical channels, and the coefficients A, E_{TF} and E_{th} are given in [17]. E_0 and α are the energy and the impinging angle of the absorbed particle. The sputtered C atoms are Maxwell distributed with 2 eV temperature.

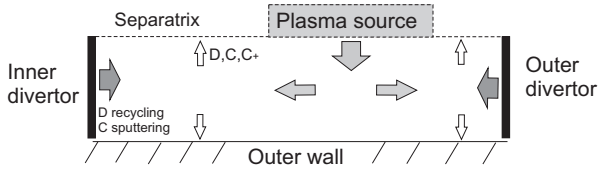

Fig. 1. Simulation geometry.

The recycling coefficient for D due to D, or D^+ impact on carbon divertor surface is given as:

$$R = \frac{0.99(1 + 0.5(E_0/200)^{1.5})}{1 + 0.5(E_0/200)^{1.5} + 0.1(E_0/200)^2}. \quad (4)$$

This choice has been made after large number of test runs. In the stationary SOL the effective recycling coefficient (including D_2 channel) is of the order of 0.99. Applying the same coefficient to the ELMy SOL results in an extremely high D density (to 3.5×10^{20} m^{-3}) in front of the outer divertor, so that after 200 μs more than 60% of the energy is carried to the divertor plates by the charge-exchanged D atoms. These results are not observed at the experiment indicating that probably the effective recycling coefficient for high energy D^+ ions is much lower. The coefficient (4) takes into account this fact: for energies above 200 eV it reduces to the values given in [18].

ii. We added a heat source, enabling simulation of high recycling SOL when the energy flux through the separatrix is "conductive", i.e. carried mainly by anomalous heat transport. In the simulation this heat source represents imaginary collisions with some medium with fixed temperature [19]. Poloidal position of the heat source agrees with the particle source. "Collision" strength for the stationary SOL corresponds to thermal conductivity $\chi_\perp \approx 0.1\, n(\mathrm{ms})^{-1}$, where the scale length of the cross-field gradient (δr) is assumed to be $\delta r \approx 1$ cm. In the ELMy SOL the heat source is switched off.

iii. In order to mimic impurity (C^+) diffusion from the simulated flux tube some of C^+ – electron pairs are removed from the simulation. The number of removed pairs (per time step) corresponds to the diffusion coefficient $D_\perp \sim 1\mathrm{m}^2/\mathrm{s}$.

All simulations have been performed on HECTOR (Edinburgh, UK) and HPC-FF (Julich, Germany) supercomputers. Times required for stationary and ELMy SOL simulations on 512 processors are about 36 and 24 h, respectively.

3. The stationary (inter-ELM) SOL

We have simulated three different SOLs with different collisionalities corresponding to high, moderate and low plasma densities. The latter corresponds to a non-recycling SOL without neutrals and impurity. The temperature and the density profiles in the outer divertor plasma are given in Fig. 2a and b. In the same figures are shown the corresponding simulated and real TP measurements. The latter is taken from the TP probe 20 (JET shot #74380), which is located near the strike point. In order to take into account a possible uncertainty with the poloidal position of the probe we consider two positions: one at 1.6 mm and another at 0.3 mm from the divertor surface. As one can see the TP measures T_e precisely for low and high collisionalities, while the measured n is somehow inaccurate. The reason for this inaccuracy is the assumption for the ion sound speed given in Eq. (1), which may be too rough. As it was expected, the simulated TP measurements are insensitive to the choice of the biasing potential U, provided that $eU \gg T_e$ (see Fig. 3).

The situation is different for moderate collisionalities: the TP overestimates significantly the actual temperature and moreover, the actual temperature profile is not monotonic any more. These effects are consequence of deviation of the EVDF from the Maxwellian. In Fig. 4a are shown the EVDF at the position of the TP for different collisionalities. The EVDF for high collisionality coincides with the Maxwellian (within the given accuracy) and can be used as a reference distribution. The EVDF for the low collisio-

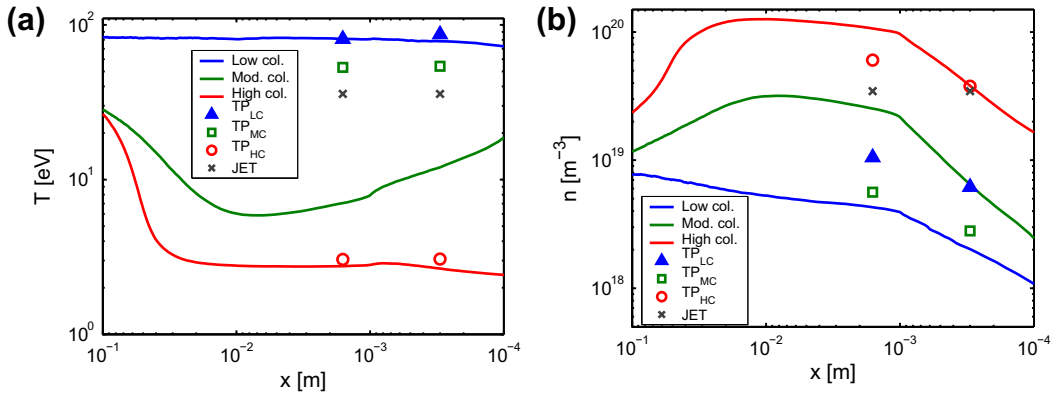

Fig. 2. Poloidal profiles of the electron temperature (a) and the density (b) in the outer divertor plasma. "Low col.", "Mod. Col." and "High col." denote direct output (i.e. actual T_e) for low, moderate and high collisionalities. "$TP_{L,M,H}$" and "JET" denote the corresponding simulated and experimental TP measurements. Here and below $x = 0$ corresponds to the outer divertor surface.

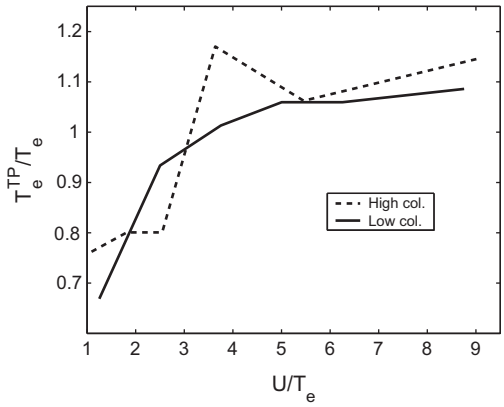

Fig. 3. Normalized simulated TP temperature vs. normalized biasing potential.

nality case well agrees with the cut-off Maxwellian distribution, which is expected in front of the divertor plate. Contrary to this the EVDF for the moderate collisionality shows a high energy tail. The reason of this deformation is different collisionality of the thermal and super-thermal electrons: the thermal electrons suffer inelastic collisions with the neutrals and impurity, as well as Maxwellizing Coulomb collisions. This leads to effective cooling of this fraction, when the corresponding VDF is still near to the Maxwellian, but with lower temperature, T'_e. Contrary to this, the super-thermal electrons are in (Coulomb-) collisionless regime and the corresponding VDF deviates from the Maxwellian with $T = T'_e$. As it was mentioned in [10], the LP are very sensitive to the presence of non-Maxwellian super-thermal electrons, which as we see leads to the overestimation of measured T_e.

The value of deformation of the EVDF is defined by the relative rate of de-Maxwellizing (inelastic) and Maxwellizing (Coulomb) collisions. In Fig. 5 are shown mean-free-paths of electron inelastic (l_{in}) and Coulomb (l_c) collisions for typical divertor plasma parameters. This figure shows that the EVDF can be divided into two parts: low and high energy fractions suffering mainly Maxwellizing and de-Maxwellizing collisions, respectively. For low and high collisional cases considered above most of the electrons belong to the first fraction, while for the case of moderate collisionality both fractions are present causing deformation of the EVDF.

Temperatures measured by the real and the simulated probes in the case of moderate collisionality agree well (see Fig. 2a). There is a good agreement in experimentally measured density and the density from PIC too (see Fig. 2b), convincing that the simulated SOL with moderate collisionality corresponds to the inter-ELM SOL from the shot #74380. Hence, the real TP probably overestimates the actual temperature just as the simulated.

4. The ELMy SOL

The ELM is simulated by increasing the strength of the particle source and the temperature of the incoming particles, $T^0_{e,i}$. For simulation we choose the shot #74380 with well-diagnosed T_e and

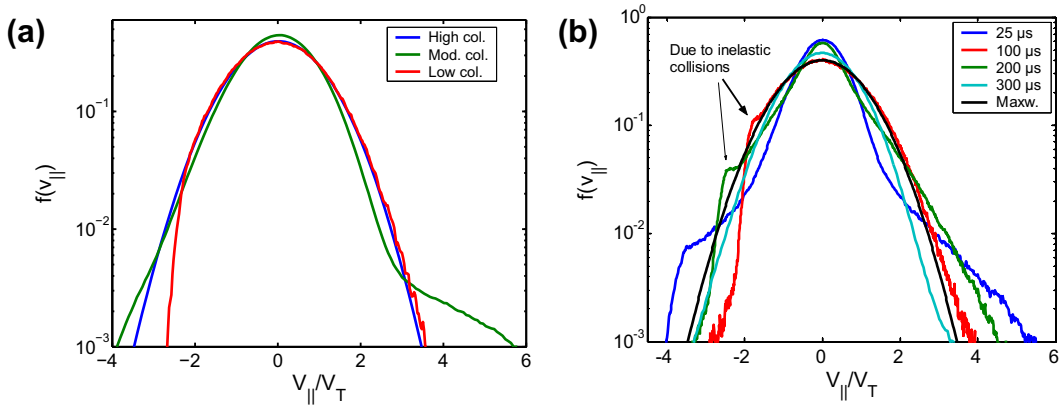

Fig. 4. Normalized EVDFs ($\int_{-\infty}^{\infty} f_e dV_{\|} = 1$) at the position of a TP ($x = 1.6$ mm). (a) For stationary SOL with different collisionalities; (b) for ELMy SOL at different times after starting of the ELM.

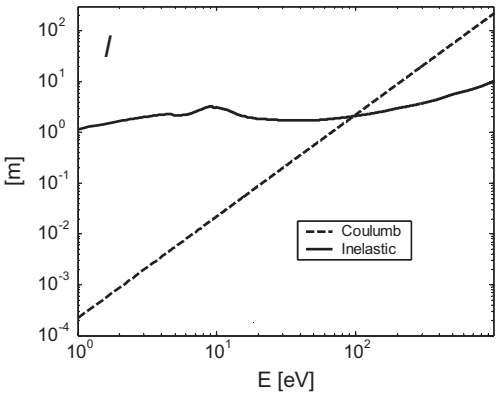

Fig. 5. Mean free paths for electron inelastic and Coulomb collisions (l) vs. the electron energy. Following inelastic collisions are considered: excitation, ionization and dissociation collisions with D, D_2, C and C^+. Atomic data are used from [20–22]. Plasma, atomic, molecular and impurity densities are chosen as $n_e = 2 \times 10^{19}$, $n_D = 10^{19}$, $n_C = n_{C^+} = 2 \times 10^{18}$ and $n_{D_2} = n_{D_2^+} = 5 \times 10^{18}$ [m^{-3}].

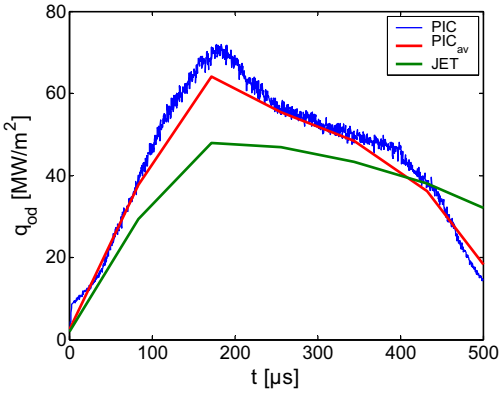

Fig. 6. Power flux to the outer divertor plate during the Type-I ELM from simulation and IR-thermography (shot #74,380). Here and below PIC_{av} denote PIC results averaged over 100 μs.

power flux to the divertor. Simulation parameters are chosen according to the experimental observations: $T_e^0 = T_e^{ped} = 720$ eV, $T_i^0 = T_i^{ped} = 1.2$ keV, the ELM source has a rectangular shape in time (see [9]). Duration of the ELM source, $\tau_{ELM} = 400$ μs, is chosen for better matching of power loads to the outer divertor measured by IR-thermography (see Fig. 6). Time resolution of PIC simulation

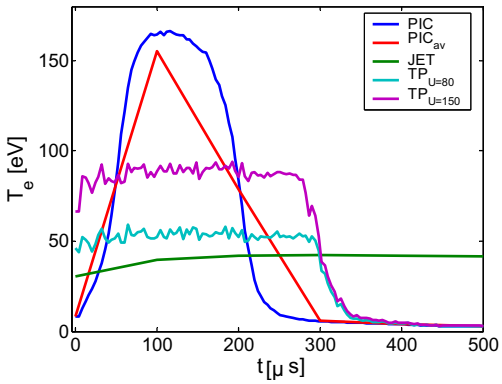

Fig. 7. Electron temperature at the position of the TP (at $x = 1.6$ mm) during the Type-I ELM (shot #74,380). "PIC", "TP_U" and "JET" denote results obtained from PIC and measured by simulated and real TPs, respectively.

is orders of magnitude higher than resolution of TP diagnostic (which is about 100 μs). Hence, for comparison with the experiment the PIC results are averaged over 100 μs.

In Fig. 7 is plotted time evolution of the electron temperature from PIC simulation together with the corresponding simulated and real TP measurements. Here and below the experimental measurements correspond to the coherent averaged Type-I ELM. As one can see the TPs underestimate significantly the actual T_e during the first 200 μs. Later, the actual T_e reduces below the inter-ELM values. The T_e form the simulated TPs follows the actual one with some delay, while the experimentally measured T_e stays almost unchanged (within 500 μs). The simulation results can be easily explained by the fact that after 200 μs the recycled neutral and sputtered impurity densities increase strongly and cause cooling of electrons in the divertor plasma. We note that the condition $eU \gg T_e$ during the ELM is not satisfied any more, so that measured temperature depends on biasing voltage (see Fig. 7). In Fig. 3b are plotted EVDF at different times, demonstrating strong deviation from the Maxwellian for $t < 200$ μs. Later due to extremely high plasma density ($\sim 10^{20}$ m^{-3}), which is forming in front of the divertor plates, plasma becomes collisional, so that the EVDF relaxes to Maxwellian. Although the EVDF becomes near-Maxwellian the TP still underestimates T_e until it reduces sufficiently, so that the condition $eU \gg T_e$ starts to satisfy.

It is important to note that PIC simulation shows significantly lower J_{sat}^i (by the factor ~5) than one measured experimentally. As a result, the density estimated in the experiment from Eq. (1) is higher than density obtained from the simulation (see Fig. 8a and b). It is interesting to note, that the divertor heat loads ob-

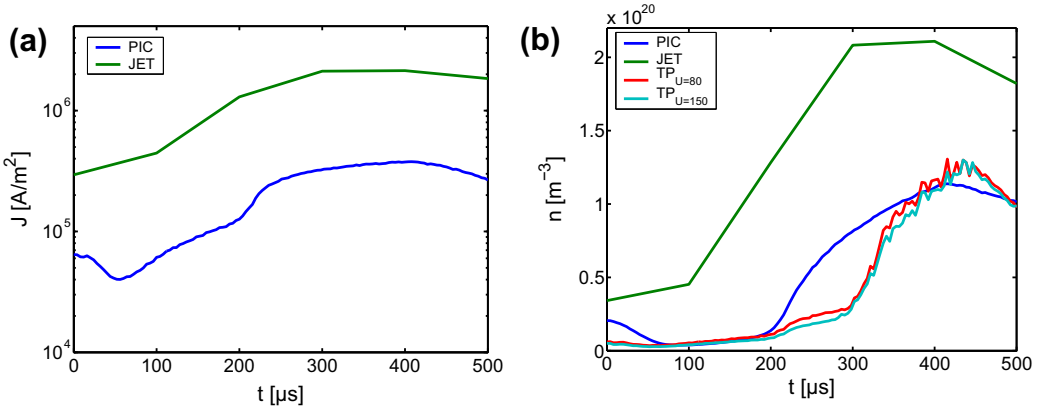

Fig. 8. Ion saturation current (a) and plasma density obtained from PIC and TPs using Eq. (1) (b). The notations are same as for Fig. 7.

tained from experimental TPs (using Eq. (1)) can still reasonably well reproduce the IR-thermography. The reason is that according to Eq. (1) $q_{div} \sim J^i_{sat} T_e$, where J^i_{sat} and T_e are over/under estimated roughly by the same factors.

5. Conclusions

Our simulations indicate that the realistic EVDF in the divertor plasma can strongly deviate from Maxwellian. The origin of this deviation in the stationary SOL is the inelastic collisions. As a result, under some circumstances, e.g. for moderate divertor plasma collisionalities, TPs can overestimate the actual T_e by the factors up to five. Contrary to this, TPs seem to underestimate peaking values of T_e during the ELMs up to 70%. There are two reasons for this: (i) in the ELMy SOL the additional de-Maxwellizing factor is the existence of two electron fractions: the thermal and hot electrons generated by the ELM; (ii) the condition $eU \gg T_e$ is not satisfied.

Acknowledgements

This work was supported by EURATOM and carried out within the framework of the European Fusion Development Agreement. The views and opinions expressed herein do not necessarily reflect those of the European Commission. The first author acknowledges support by the Projects P21941-N16, TW9-TGS-01-06, GNSF/ST09_305_4-140, EFDA ITM-EUFORIA and DEISA.

References

[1] V.I. Demidov, S.V. Ratynskaia, K. Rypdal, Rev. Sci. Instrum. 73 (10) (2002) 3409.
[2] D. Tskhakaya, S. Kuhn, V. Petržílka, R. Khanal, Plasmas 9 (6) (2002) 2486.
[3] G. Fussmann, U. Ditte, W. Eckstein, et al., J. Nucl. Mater. 128–129 (1984) 350.
[4] J. Horacek, R.A. Pitts, P.C. Stangeby, et al., J. Nucl. Mater. 313–316 (2003) 931.
[5] A. Herrmann, T. Eich, S. Jachmich, et al., J. Nucl. Mater. 313–316 (2003) 759.
[6] A. Kallenbach, Y. Andrew, et al., Plasma Phys. Contr. Fusion 46 (2004) 431.
[7] S. Jachmich, Y. Liang, G. Arnoux, et al., J. Nucl. Mater. 390–391 (2009) 768.
[8] R.A. Pitts, P. Andrew, G. Arnoux, et al., Fusion 47 (11) (2007) 1437.
[9] D. Tskhakaya, R.A. Pitts, W. Fundamenski, et al., J. Nucl. Mater. 390–391 (2009) 335.
[10] P.C. Stangeby, Plasma Phys. Contr. Fusion 37 (1995) 1031.
[11] T. Van Rompuy, J.P. Gunn, R. Dejarnac, et al., Plasma Phys. Contr. Fusion 49 (2007) 619.
[12] M. Cercek, T. Gyergyek, B. Fonda, et al., J. Plasma Fusion Res. Series 8 (2009) 381.
[13] D. Tskhakaya, R. Schneider, J. Comp. Phys. 225 (1) (2007) 829.
[14] D. Tskhakaya, A. Soba, R. Schneider, et al., In: Proceedings of the 18th Euromicro Conference on Parallel, Distributed and Network-based Processing, Pisa, Italy, 2010, p. 476.
[15] D. Tskhakaya, F. Subba, X. Bonnin, et al., Contrib. Plasma Phys. 48 (1–3) (2008) 89.
[16] D. Tskhakaya, S. Kuhn, Y. Tomita, et al., Contrib. Plasma Phys. 48 (1–3) (2008) 121.
[17] J. Bohdansky, Nucl. Fusion (1984) 61 (special issue).
[18] W. Eckstein, H. Verbeek, Nucl. Fusion (1984) 12 (special issue).
[19] D. Tskhakaya, S. Kuhn, Contrib. Plasma Phys. 42 (2–4) (2002) 302.
[20] R.K. Janev (Ed.), Atomic and Molecular Processes in the Fusion Edge Plasmas, Plenum Press, New York and London, 1995.
[21] R.K. Janev, D. Reiter, U. Samm, FZJ report, 2003.
[22] H. Suno, T. Kato, NIFS_DATA_91, 2004.